Fishtail shape in the magnetic hysteresis loop for superconductors: Interplay between different pinning mechanisms

M. Jirsa, L. Půst, and D. Dlouhý
Institute of Physics, Academy of Sciences of the Czech Republic, Na Slovance 2, CZ-18040 Praha 8, Czech Republic

M. R. Koblischka
Groupe de Physique Appliquée, Université de Genève, 20, Rue d'Ecole de Médecine, CH-1211 Genève 4, Switzerland
(Received 10 January 1996)

The scaling and relaxation behavior around the fishtail minimum is studied in detail in a wide temperature range (3–70 K) on $DyBa_2Cu_3O_{7-\delta}$ single crystals exhibiting a pronounced fishtail effect. Magnetic hysteresis loops (MHL's) normalized with respect to the height and position of the fishtail maximum fall on a universal curve which form can be derived from the phenomenological model of a thermally activated flux creep proposed by Perkins *et al.* [Phys. Rev. B **51**, 8513 (1995)]. This universal curve tends at low fields towards zero. At low temperatures, the drop of j_s at low fields is usually masked by a wide central peak. By subtracting the universal curve from the experimental $j_s(B)$ data we separate the contribution of the central peak. It has a simple, exponentially decaying field dependence. This implies that the fishtail minimum at low fields might be understood as a result of an overlapping of two contributions originating from separate pinning mechanisms: one active mainly at high fields and dying away with B going to zero and another one (responsible for the central peak of the MHL) vanishing rapidly with increasing field. This concept is also supported by relaxation experiments. These experiments confirm that the shape of MHL's is given by a dynamic equilibrium between the induction, pinning, and relaxation processes. [S0163-1829(97)05305-8]

I. INTRODUCTION

The fishtail effect, a special shape of the magnetic hysteresis loop (MHL), was observed many years ago on bulk samples of conventional (low-T_c) superconductors.[1–3] The discovery of the high-temperature superconductors (HTSC's) has led to a revival of interest in this phenomenon as most of the HTSC bulk samples exhibit this effect, too.[4–9] The fishtail effect is widely discussed in the literature and many new ideas are proposed.

One approach argues that the fishtail deformation of the MHL is due to an anomalous increase of the critical currents at high fields resulting from an additional pinning on nonsuperconducting particles becoming active at high fields. As regards the origin of these particles, there are many proposals: zones with a lower second critical field[3] B_{c2}, field-induced granularity,[5] oxygen vacancies changing the pinning efficiency at higher fields,[6] and others being more sample specific.[10] One of the oldest hypotheses explaining the fishtail maximum by matching the mean vortex lattice constant to the mean distance between pinning sites belongs to this family, too.

Krusin-Elbaum *et al.*[9] proposed a dynamic explanation based on the observed enhanced creep in the vortex system in the vicinity of the fishtail minimum. It attributes the minimum to a crossover between two pinning regimes, namely, between the domain of single vortices and the domain of vortex bundles. The consequences of this model, which should be valid quite generally, contradict, however, many experiments. The most striking difference is in the field dependence of the normalized logarithmic relaxation rate $S(B)$ which in experiments does not mirror the shape of the MHL at the fishtail minimum as proposed.[7] The low-field maximum of $S(B)$ is observed in our and many other samples[11] at fields *below* the fishtail minimum.

The enhanced sensitivity of the induced magnetic moment to the field sweep rate in vicinity of the fishtail minimum was pointed out in Ref. 7. These experimental data were analyzed in Ref. 12 by means of the generalized inversion scheme (GIS) proposed recently by Schnack *et al.*[13]

The calculation of the ''real'' critical current density j_0 by extrapolating the experimental data on the measured current density $j_s(T)$ and $S(T)$ to zero temperature[12] showed that the field dependence $j_0(B)$ does not exhibit the fishtail shape. This important result points clearly to the dynamic character of the fishtail phenomenon.

Perkins *et al.*[11] showed the close correlation between the shape of the MHL and the relaxation rate. The analysis proposed in Refs. 11 and 14 enables one to determine the temperature and field dependences of the effective pinning barrier in the sample exhibiting the fishtail effect.

In spite of the large amount of theories proposed until now none of them is capable of a satisfactory description of all the experimental observations connected with the fishtail phenomenon. The potential solution of the fishtail problem has to bring into harmony the both still contradictory approaches, the static and the dynamic one, each of them supported by the extensive reliable experimental material. It also needs to explain why some samples exhibit this effect and others do not, the differences in the fishtail shapes observed in different families of superconducting materials [conventional superconductors, R-Ba-Cu-O ($R \equiv$rare earth), Bi-Sr-Ca-Cu-O], and many other questions.

We believe that the ''fishtail problem'' cannot be restricted only to the ''anomalous'' MHL's but that it is a general problem of the understanding of the MHL shape at

all. The preceding relaxation experiments point to the importance of the central peak region in connection with the appearance of the fishtail minimum. Therefore, we focus in this paper on the scaling properties of the MHL and to the relaxation behavior at low fields around the central peak. The analysis of the experimental data is made in intention of the method proposed by Perkins *et al.*[11,14]

II. EXPERIMENTAL PROCEDURE

We used for our study $DyBa_2Cu_3O_{7-\delta}$ (DBCO) single crystals which exhibit a pronounced fishtail effect.[7,12] The experiments have been carried out on a series of six DBCO single crystals originating from the same batch grown from flux by the slow-cooling method identical with that used in Ref. 15 for preparation of $YBa_2Cu_3O_{7-\delta}$ single crystals. Magneto-optical observations proved that all the crystals were naturally twin free.

Magnetic hysteresis loops recorded at a constant field sweep rate and time-dependent relaxations of the magnetic moment were measured at various temperatures (3 K $\geqslant T \geqslant$ 70 K) by means of a vibrating sample magnetometer (VSM) PAR 155 controlled by a PC 486 which was also used for the data acquisition and processing. A magnetic field in the range $\pm$ 2 T was generated by an electromagnet with the analog sweep rate control enabling a continuous smooth field sweep. Measurements were performed with the field oriented parallel to the c axis of the samples (perpendicular geometry). Before each conventional relaxation (CR) experiment the external magnetic field was increased to the target value with a constant sweep rate $dB/dt =$ 29 mT/s.

To avoid any field overshoot, the feedback circuit of the field regulator works in the aperiodic regime. This leads to a rather long time period between the stop of the control voltage and the real stop of the magnetic field sweep. During this characteristic delay time (typically 10–12 s) the rate of the field sweep slows down from 29 mT/s to zero. During all measurements on our VSM we record simultaneously magnetic field, magnetic moment, time, and temperature. In the field sweep regime it enables us to eliminate the effect of the sweep rate on the shape of the MHL in most of the used field range. In the case of conventional relaxation, the point when the applied field gets constant can be easily determined. In this paper we set into this point the origin of the time scale, $t = 0$, for the conventional relaxation data. The decay of the induced magnetic moment M at a constant field was always measured for the same time period of 900 s.

All six measured crystals showed qualitatively the same magnetic behavior; therefore, only the results obtained on the largest one, with dimensions $a \times b \times c = 0.92 \times 1.71 \times 0.015$ mm^3, are presented in this paper. Critical temperature was $T_c =$ 87 K as determined from the zero-field cooling (ZFC) curve measured by a Quantum Design superconducting quantum interference device (SQUID) magnetometer.

The current density j_s was calculated using the extended Bean formalism which for $\vec{B} || c$ gives $j_s = \Delta M/\Omega$ where $\Omega = a^2(b - a/3)c/2$ and ΔM is the difference between magnetic moments M on the descending and ascending field branches of the MHL. For our sample $\Omega = 8.91 \times 10^{-3}$ mm^4.

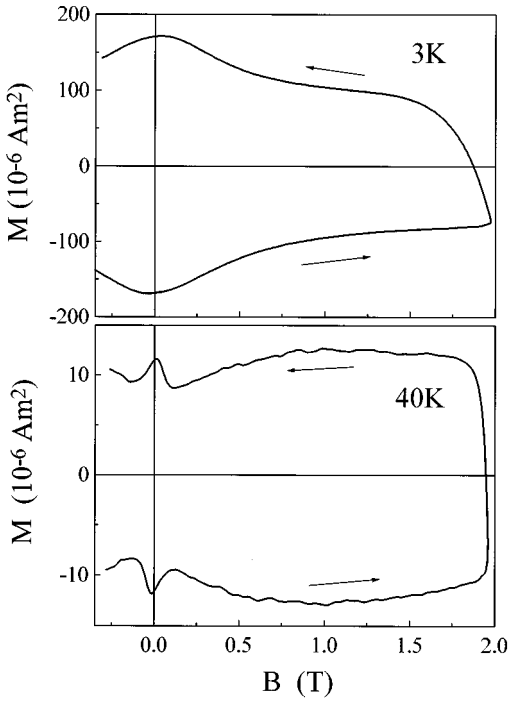

FIG. 1. Full hysteresis loops of the induced magnetic moment M as a function of external field B at $T =$ 3 K (no fishtail) and at $T =$ 40 K, where a clear fishtail shape is developed. The sweep rate is $dB/dt =$ 29 mT/s.

III. EXPERIMENTAL RESULTS

Typical shapes of the MHL's observed at low and high temperatures are shown in Figs. 1(a) and 1(b). Whereas at $T =$ 3 K [Fig. 1 (a)] the size of the MHL (difference of the magnetic moments on the ascending and descending field branches) continuously decreases with increasing field in the whole field window, the MHL measured at $T =$ 40 K [Fig. 1 (b)] shows a well-developed minimum at intermediate fields (the fishtail shape).

The temperature scan of $j_s(B)$ determined from the MHL's measured at temperatures ranging from 3 K to 70 K is presented in Fig. 2. Different j_s-axis formats used in Figs. 2(a) and 2(b) emphasize different features of the field and temperature dependences. In Fig. 2 (a) we can compare real sizes of the $j_s(B)$ curves measured at different temperatures. The significant feature of this plot is the rapid reduction of the central peak (both in height and width) with increasing temperature. The dotted line with the slope[16] $|\chi_0|/3$ indicates the field of full flux penetration, B_{pen}, approximated as $|B_{pen}| \approx 3\mu_0 M_{pen}/|\chi_0|$. χ_0 is the initial susceptibility measured as a slope of the virgin magnetization curve at zero field, μ_0 is the permeability of a free space, and M_{pen} is the magnetic moment on the MHL at the external field $B = B_{pen}$.

The starting slope of the virgin magnetization curve after the zero field cooling $\chi_0 = \mu_0 \Delta M/\Delta B$ is determined by the volume screened by the induced surface currents in the sample. For long cylindrical samples with axis parallel to the external field this volume is close to the sample volume but for a thin flat cylindrical sample with diameter d, perpendicular to field,[17] $\chi_0 = -d^3/2 \approx -(4\pi/3)(d^3/8)$; i.e., the screened volume is as large as the sphere with diameter equal

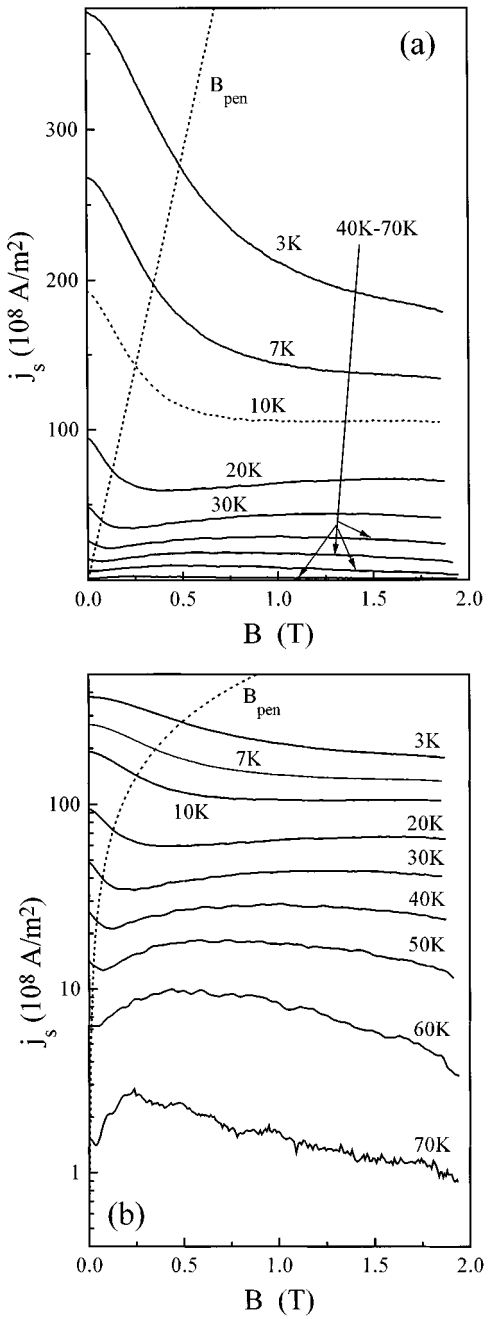

FIG. 2. Development of the fishtail effect with raising temperature in terms of the critical current density $j_s=\Delta M/\Omega$ evaluated from hysteresis loops recorded with sweep rate $dB/dt=$ 29 mT/s. The dotted line indicates the penetration field B_{pen}, approximated as $3\mu_0 M(T)/\chi_0$. The scaling of the MHL shape with B_{pen} is clearly seen for both low temperatures (a), linear scale of j_s, and high temperatures (b), logarithmic scale of j_s. In the latter plot the equidistant curves of $j_s(B)$ indicate the exponential field dependence of j_s.

to the diameter of the sample. In flat samples with other than circular geometry d should be replaced by an effective magnetic diameter of the sample plane. It means that χ_0 is a geometrical factor, nearly temperature independent (except for the temperatures in vicinity of T_c). Its value is also close to the differential susceptibility characterizing the magnetization response of the sample on small variations of the external magnetic field and the reversal of the field sweep (reverse leg). In our sample the experimental value is $\chi_0=-0.9\ \mathrm{mm}^3$, corresponding to the effective lateral diameter $d_{eff}=(2\chi)^{1/3}=1.2$ mm. It is in a good correlation with the sample dimensions $0.92\times 1.71\ \mathrm{mm}^2$.

We see that the width of the central peak of the MHL scales well with B_{pen}. As $B_{pen}\propto M\propto j_s$ (Ref. 16), it is natural to expect decrease of the central peak width with increasing temperature proportional to j_s. The logarithmic plot of j_s in Fig. 2(b) shows that the $\ln[j_s(B)]$ curves are nearly equidistant in a wide temperature range. It means that j_s decreases exponentially with increasing temperature (only above 50 K this dependence becomes more pronounced). Consequently, the central peak width decreases exponentially with temperature, too.

Simultaneously with the reduction of the central peak, the fishtail develops from a classical, monotonously decreasing curve at low temperatures through a shallow and wide minimum observed on MHL's at around 10 K up to a deep and narrow minimum observed at high temperatures. The position of the minimum shifts with raising temperature to lower fields. We note that the fishtail dip lies consistently outside but close to the border of the field range delimited by the B_{pen} values.

For temperatures above 10 K where the fishtail peak can be recognized and its position B_p and height j_p can be directly measured the experimental data of the Fig. 2 were normalized with respect to the fishtail peak coordinates (B_p, j_p). The normalized curves $j_{sc}(B_{sc})$ where $j_{sc}=j_s/j_p$ and $B_{sc}=B/B_p$, are plotted in Fig. 3(a).

The MHL curves for low temperatures exhibiting explicitly no fishtail maximum were normalized with the help of the B_p and j_p values obtained by extrapolation from high temperatures [Figs. 4(a) and 4(b)]. A fit of these data showed that $B_p(T)=2.2(1-T/T_c)^{1.37}$ T and $j_p(T)=1.67\times 10^{10}\exp(-T/22.2K)\ \mathrm{A/m}^2$. In Fig. 4(b) the temperature dependence $j_p(T)$ is compared to the temperature development of the central peak height, $j_{cp}(T)$. It was found that j_{cp} scales with temperature as $j_{cp}(T)=3.767\times 10^{10}\exp(-T/14.6K)\ \mathrm{A/m}^2$. The preexponential coefficients in $j_p(T)$ and $j_{cp}(T)$ represent the values extrapolated to zero temperature. Addition of the normalized low-temperature data into Fig. 3 is not important for the presentation of the high-field range scaling (which is better demonstrated by the high-temperature measurements) but it is crucial for the analysis of the central peak scaling discussed below.

The reduction of the central peak with increasing temperature could imply that the shape of the high-field pinning regime could be even better documented by the experimental data at temperatures above 70 K. However, we found that the character of the pinning and depinning processes at temperatures close to T_c changes and it cannot be described consistently within the approach presented in this paper. Due to the very low magnitude of the induced magnetic moment in this temperature range, there is also a high scatter in the experimental data recorded by the VSM.

Dynamic properties of the vortex system in different fields and temperatures were investigated by means of the conventional relaxation measurement. For the sake of comparability between individual measurements all the relax-

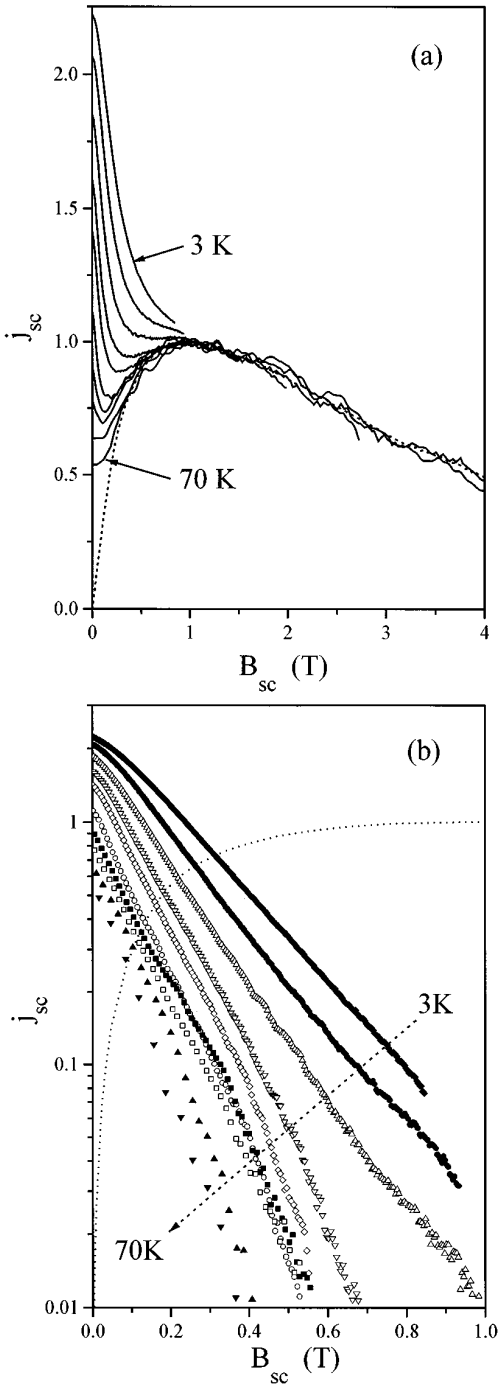

FIG. 3. (a) Normalized critical current densities j_s/j_p for different temperatures as a function of the normalized field $B_{sc}=B/B_p$. The universal curve given by Eq. (4) with $m=1$ and $n=0.5$ is shown as a dotted line. (b) The same experimental data as in (a) after subtraction of the universal curve [the concave dotted line in (a)]. We note the linear field dependence of the central-peak component of the scaled current density which corresponds well to the dependence described by Eq. (7).

ations were recorded for the same time of 900 s starting from the moment of a real field stabilization. The results are summarized in Fig. 5 in the $M(B)$ representation which enables us to compare both the relaxation rate at different fields and the whole relaxation process with respect to the size of the magnetization loop from which all relaxations had started.

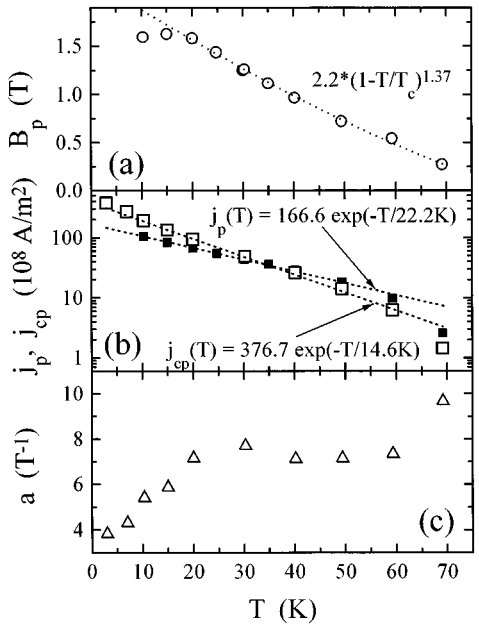

FIG. 4. The temperature dependences of the position of the fishtail peak, B_p (a), of the heights of the high-field (fishtail) and central peaks of MHL, j_p and j_{cp}, respectively (b), and of the coefficient a in the exponential field dependence of the central peak, Eq. (7) (c).

The strength of the relaxation is symbolized by the difference between the current density at the beginning [the lowest point $M(t\approx 0)$] and at the end [the highest point $M(t\approx 900$ s)] of each relaxation indicated in Figs. 5(a) and 5(b) by

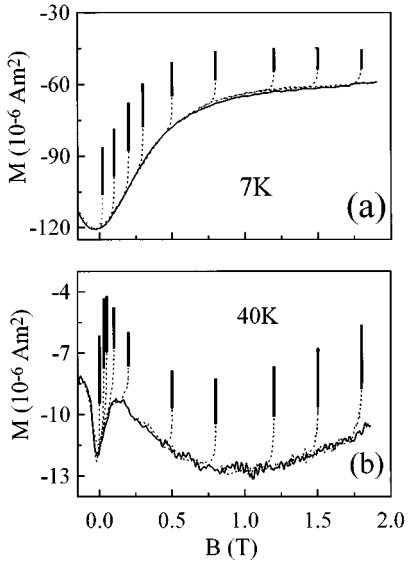

FIG. 5. Conventional relaxation (CR) measurements represented by magnetic moment as a function of magnetic field $M(B)$ (solid vertical lines) for two temperatures $T=$ 7 K (a) and 40 K (b). All the CR's were recorded up to $t=$ 900 s. From the evolution of the applied field with time the starting point of each CR (the lowest point of the solid line) was determined as the time for which the applied field became constant after transition (dotted line) from the preceding constant-sweep mode (MHL). This time was set as an origin for analysis of the CR data.

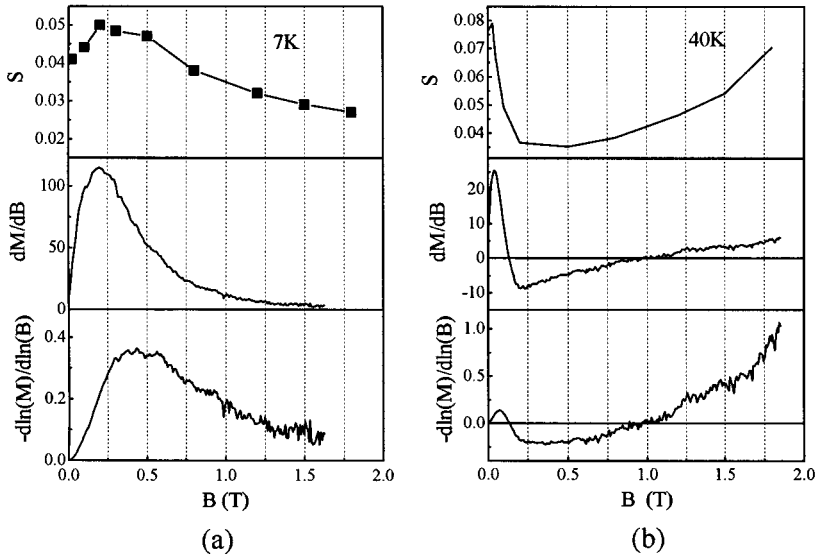

FIG. 6. Comparison of the field dependences of the logarithmic relaxation rate $S=-d\ln|M|/d\ln t$, slope of the MHL, $d|M|/dB$, and the logarithmic susceptibility $\chi_{\ln}=d\ln|M|/d\ln B$ for two temperatures $T=$ 7 K (a) and 40 K (b).

thick vertical line. The dotted lines connecting the individual relaxations with the MHL correspond to the field-sweep-damping process. All the conventional relaxations were measured on the positive ascending field branch of the hysteresis loop (where M is negative).

Comparison of Figs. 5(a) and 5(b) shows that the character of relaxation is strongly temperature dependent: In both indicated temperatures 7 K and 40 K, the creep rate culminates close to zero field and then decreases with increasing field. At 7 K [Fig. 5(a)] the decrease is slow but continuous up to 2 T, at $T=$ 40 K [Fig. 5 (b)] the decrease is sharp but stops at $B\approx 0.3$ T and then the creep rate starts to grow again.

The relaxation process can be quantitatively characterized by the logarithmic relaxation rate $S=-d\ln(M)/d\ln(t)$. The field dependence of S is shown in Figs. 6(a) and 6(b) for 7 K and 40 K, respectively. These dependences confirm the relaxation characteristics from Figs. 5(a) and 5(b) and show correlation between the dynamic processes in the vortex lattice and the shape of the MHL. This correlation was found between S and the simple or logarithmic derivative of M (called the logarithmic susceptibility), $d|M|/dB$ or $\chi_{\ln}=-d\ln|M|/d\ln(B)$, respectively.

IV. DISCUSSION

A. MHL scaling

Analysis of the scaling properties of MHL's around and above the fishtail maximum presented in this paper is based on the model proposed by Perkins *et al.*[11,14] This model is constructed assuming only the thermally activated creep process. It means that the effective electric field induced in the sample by change of the current density with time is

$$E=B\omega d\,\exp\left[\frac{-U_{\rm eff}(j_s,B,T)}{kT}\right], \tag{1}$$

where ω the microscopic attempt frequency, d the effective vortex jump distance, $U_{\rm eff}$ is the effective activation energy, and k is the Boltzmann constant. Following Schnack *et al.*[13] and Perkins *et al.*,[11,14] the effective activation energy $U_{\rm eff}$ is chosen in the form

$$U_{\rm eff}(j_s,B,T)=U_0(B,T)V\left[\frac{j_s}{j_0(B,T)}\right], \tag{2}$$

where the functional dependence of $U_{\rm eff}$ on the current density is formally separated into the function V. U_0 and j_0 are the characteristic parameters of the creep process.

The empirical scaling of $j_s(B)$ curves presented in Fig. 5(a) implies that in the high-field region the normalized current density $j_{\rm sc}$ is a function of only the normalized field $B_{\rm sc}$, $j_{\rm sc}=\Phi(B_{\rm sc})$; i.e., all the temperature dependence of $j_{\rm sc}$ is included only in the temperature dependencies of j_p and B_p.

In Eq. (2) we can replace $U_{\rm eff}$ by $kT\ln(B\omega d/E)$ [see Eq. (1)]. It is useful to express j_0 and U_0 as products of the temperature- and field-dependent terms,[11] $j_0(B,T)=\Lambda(T)B^m$ and $U_0(B,T)=\Psi(T)B^{-n}$. The temperature functions $\Lambda(T)$ and $\Psi(T)$ can be determined from the fishtail coordinates as follows:[14]

$$\Lambda(T)=\lambda j_p(E,T)B_p^{-m}(E,T),$$

$$\Psi(T)=\psi\ln(B\omega d/E)TB_p^n(E,T), \tag{3}$$

where λ and ψ are constants. Perkins *et al.*[11,14] have found for $TmBa_2Ca_3O_7$ single crystals that $V\propto ln(j_s)$. Taking into account the logarithmic character of the function V, Eq. (2) can be rewritten as $j_{\rm sc}(B_{\rm sc})=\lambda B_{\rm sc}^m\exp[(-k/\psi)B_{\rm sc}^n]$. Such a function of $B_{\rm sc}$ has a form appropriate for the description of the experimentally found scaling. However, to fit the scaled data, this dependence has also to satisfy two boundary conditions at $B_{\rm sc}=1$, namely, $dj_{\rm sc}/dB_{\rm sc}=0$ and $j_{\rm sc}=1$. These conditions exert constraints on the constants λ and ψ: $\lambda=\exp(k/\psi)$, $\psi=kn/m$. With these values the $j_{\rm sc}(B_{\rm sc})$ reads

$$j_{\rm sc}(B_{\rm sc})=B_{\rm sc}^m\exp\left[\frac{m}{n}(1-B_{\rm sc}^n)\right]. \tag{4}$$

In Ref. 11, the authors found, for $TmBa_2Cu_3O_7$, $m=n=1$. The function from Eq. (4) with $m=n=1$ fits the

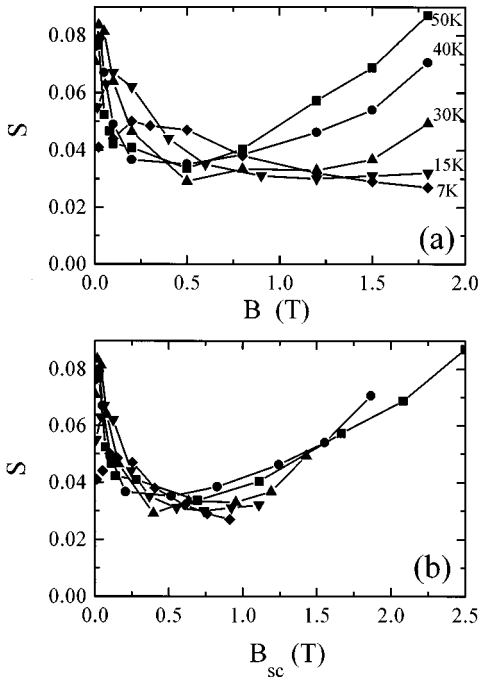

FIG. 7. The logarithmic relaxation rate S as a function of the applied field B (a) and the scaled field $B_{sc}=B/B_p$ (b) for temperatures ranging from 7 K to 50 K.

scaled experimental data in Fig. 3(a) reasonably well at low fields, $B_{sc}\leqslant 1$; however, in fields above the fishtail maximum it decreases too fast compared to experimental data. To obtain a better fit in the whole investigated range of fields we used n as a variable.[21] A good fit to our experimental data in the whole investigated field range was obtained with $m=1.01$ and $n=0.5$. Such a fit function is indicated in Fig. 3(a) by the dotted line.

Equation (4) is an alternative to the function $j_{sc}(B_{sc})=B_{sc}^{p}(1-B_{sc})^{q}$ used commonly in the literature.[18] Irrespective of the actual values of the parameters (m,n) or (p,q), Eq. (4) fits the experimental data better, especially at high fields.

It is likely that both the shape of the universal curve at high fields and the corresponding values of m and n are specific to each sample and are determined by a distribution and type of the microscopic pinning sites in the sample. By an artificial change of the distribution and quality of the pinning sites as done, e.g., by a variation of oxygen content or by an irradiation of the samples, the shape of the universal curve can be significantly modified.

Irrespective of the actual values of m and n, Eq. (4) describes the experimentally observed form of MHL's which is a result of different field dependences of $j_0(B)$ and $U_0(B)$, one increasing and the other decreasing with increasing field. Each of these functions plays a dominant role in a different field range (see Fig. 7 in Ref. 11). It explains the existence of the fishtail maximum and the drop of $j_s(B)$ at $B\leqslant B_p$. The temperature dependence of the depth and position of the fishtail minimum is a result of the interplay between the high-field pinning regime studied in this section and the pinning regime of the central peak range which, as will be shown below, has a quite different temperature dependence.

B. Dynamics of the vortex lattice

As shown empirically in Sec. III, the relaxation rate is correlated with the MHL shape through the simple or logarithmic derivative of M. We point out that both these quantities are related as

$$\chi_{ln}=-\frac{B}{|M|}\frac{d|M|}{dB}, \tag{5}$$

which means that the slope of the MHL, $d|M|/dB$, and the logarithmic derivative χ_{ln} are equal to zero at the same values of B (except $B=0$).

For a thermally activated vortex motion Perkins *et al.*[11] established the theoretical relation between $Q=d\ln|M|/d\ln(dB/dt)$, the logarithmic relaxation rate of the field-sweep mode (dynamic relaxation),[19] and the logarithmic susceptibility χ_{ln},

$$Q(B,E,T)=\gamma_E(E,T)[k_E(E,T)-\chi_{ln}(B,E,T)], \tag{6}$$

where γ_E and k_E are functions of temperature T and electric field E across the sample generated by the field sweep and are related[11,14] to m and n as $m=k_E$ and $n=(1-\gamma_E)/[\gamma_E\ln(B\omega d)]$.

Because the field-sweep relaxation ($dB/dt=$ const) and the conventional relaxation ($B=$ const) regimes are fully compatible[19,20] as well as the corresponding normalized relaxation rates $Q=d\ln|M|/d\ln(dB/dt)$ and $S=-d\ln|M|/d\ln(t)$, Eq. (6) can be also used for the conventional relaxation. We can therefore replace Q in Eq. (6) by S.

Following Eq. (6) we plotted experimental values of S as a function of $-\chi_{ln}$ and obtained values of $k_E\approx 1.1$ and $\gamma_E\approx 0.04$. According to this, we obtained for our sample $m\approx 1.1$, in good agreement with the value obtained in the preceding subsection. Determination of n failed due to the uncertainty in the extrapolation of $-\gamma_T(T)=-d\ln(j_p)/d\ln(B_p)$ to $T=0$ which was used in Ref. 11 for estimation of $\ln(B\omega d)$.

We will look in more detail at the $S(B)$ dependences plotted for different temperatures in Fig. 7(a). Scaling of the experimental current densities with the fishtail peak coordinates (B_{sc},j_{sc}) shown in Fig. 3(a) and the correlation between the logarithmic relaxation rate and the shape of the MHL discussed above imply that the logarithmic relaxation rate should scale with B_{sc}, too. A plot of S as a function of the normalized field is shown in Fig. 7(b). All data measured at temperatures 7–50 K fall onto one universal curve having its minimum ($S\simeq 0.027$) at the scaled field $B_{sc}\simeq 0.75$. This is a value close to the inflection point of the universal magnetization curve. It is additional proof of the correlation between creep processes and the shape of the hysteresis curve.

Figures 5(a), 6(a) and 7(a) show that at low temperatures the relaxation rate decreases at high fields continually up to the end of our experimental field range. However, even at low temperatures, one would expect a high relaxation rate at sufficiently high fields, in the vicinity of the irreversibility line. Figure 7(b) indicates that at low temperatures the upper limit of our experimental field range is below $0.75B_p$ which means that our field window is too narrow to observe the

minimum of S. We believe that at sufficiently high fields we would obtain a turnover in the $S(B)$ dependence above which S would grow with increasing field in similar manner as we observe at high temperatures.

The $S(B)$ dependence has at low fields a sharp high maximum at high temperatures which with decreasing temperature reduces rapidly and becomes flat. This process is well recognized in Fig. 7(a), somewhat worse in Fig. 7(b). Extrapolating this process to even lower temperatures, one can expect that the low-field maximum will disappear at all and will transform into a plateau with a characteristic low limit value (in our sample we observe this limit to be $S \approx 0.027$).[22]

It is interesting to note that the $S(B)$ increasing with field is observed also in thin films and tapes where the central peak dominates the low-field range similarly as in our sample at low temperatures.

The enhanced relaxation at low fields observed as a maximum on the $S(B)$ dependence may have an origin in specific conditions existing in this field region. Let us assume the sample exposed first to the external field higher than $2B_{\mathrm{pen}}$. If the applied field is then reduced to zero, the internal field is zero at the sample edge but it is approximately equal to B_{pen} at the center. B_{pen} is approximately the upper limit of the variation of the local field inside the sample. It implies that the local internal field B_{i} in some part of the sample can be zero only for $|B| \leqslant |B_{\mathrm{pen}}|$. If it is the case, i.e., if there is a part of the sample with $B_{\mathrm{i}} = 0$, vortices on opposite sides of the zero-internal-field border are oriented in opposite directions, due to the opposite Lorentz force they are attracted to each other, and finally they can annihilate at this border, *inside* the sample. They do not need to go all the way up to the sample edge to disappear. Such a relaxation mechanism is therefore restricted only to the range of external fields between $-B_{\mathrm{pen}}$ and $+B_{\mathrm{pen}}$, i.e., to the region of the central peak [see Fig. 2 (a)]. At low temperatures the thermal excitation is reduced leading to a reduction of the peak in the $S(B)$ dependence.

There are two features of our relaxation experiments which enable us to make a clear conclusion: (i) S has a minimum value at $B \approx 0.75B_{\mathrm{p}}$, not at $B = B_{\mathrm{p}}$ as predicted by the matching effect hypothesis, and (ii) S is highest around the inflection point of the central peak, not at the position of the fishtail minimum as predicted in Ref. 9. These experimental findings exclude (i) the matching effect and (ii) the crossover between the pinning regimes of individual vortices and of the vortex bundles from the potentially correct explanations.

C. Scaling of the central peak

While the high-field parts of the experimental $j_{\mathrm{s}}(B)$ curves scale well with the fishtail peak characteristics, Fig. 3(a) manifests clearly that the low-field parts (the central peaks) exhibit a quite different dependence on temperature. Similar conclusions follow also from the scaling of the logarithmic relaxation rate S [Fig. 3(b)].

These observations lead straightforwardly to the conclusion that the pinning mechanism governing the low-field (central peak) region is quite different from that which is dominant at high magnetic fields. The former one, active at external fields smaller or comparable to the penetration field B_{pen}, is related mainly to the geometrical effects[23] and/or self-fields.[11] The latter relaxation mechanism is related to the interaction of the vortices aligned with the c axis with the actual microscopic pinning structure (in our sample most probably a random pointlike pinning structure[24]) and to the collective pinning processes. The distribution and quality of pinning sites control the pinning and the depinning processes and, consequently, the shape of MHL's at high fields. At low fields, in vicinity of $B = 0$, this mechanism loses its efficiency and the $j_{\mathrm{s}}(B)$ dependence is governed mainly by the linear dependence of $j_0(B)$ (see Sec. IV A). The physical reason for this may be a dilution of the c-axis-aligned vortex lattice at low fields.

The idea of two overlapping contributions arising from different pinning mechanisms points to the significance of the central peak in the fishtail problem: At low temperatures where the central peak is high and wide, it dominates a substantial part of the investigated field range. It masks there the drop of the ''high-field'' pinning mechanism at low fields and no fishtail is observed. With an increasing temperature the central peak rapidly reduces both in height and width which enables us to trace the actual shape of the ''high-field'' pinning mechanism up to very low fields. As this mechanism loses its efficiency at low fields, one can observe a minimum separating the central peak from the fishtail maximum.

To learn more about the low-field pinning mechanism, we subtracted the universal curve given by Eq. (4) from the experimental data in Fig. 3(a).

The resulting curves very rapidly die out with increasing field. The logarithmic plot in Fig. 3(b) manifests that all these curves decay exponentially with B_{sc}. These experimental curves can be well fitted by

$$j_{\mathrm{sc}}(B_{\mathrm{sc}}) = j_{\mathrm{sc}}(0)\exp(-aB_{\mathrm{sc}}), \tag{7}$$

where a is a temperature-dependent parameter [see Fig. 4(c)]. As both j_{cp} and j_{p} are exponential functions of temperature [see Fig. 4(b)], $j_{\mathrm{sc}}(0) = j_{\mathrm{cp}}/j_{\mathrm{p}}$ depends also exponentially on temperature.

It should be noted that the magnitude of the central peak is in Eq. (7) represented by the zero-field current density $j_{\mathrm{sc}}(0)$. At very low temperatures (below 7 K) where the central peak is wide and its top is rather flat, this description fails at fields very close to zero. At these temperatures a better fit is therefore obtained with the value of $j_{\mathrm{sc}}(0)$ somewhat higher than the experimental one.

Figure 4(b) shows that the exponential decay of j_{cp} with temperature is faster than that of j_{p}. In other words, as temperature raises, the central peak of the MHL loses its dominant role at intermediate fields and at temperatures above $\approx$ 40 K the fishtail peak starts to dominate. The exponential dependences of both quantities become at temperatures above 60 K even more pronounced. It is probably due to melting of the vortex lattice.

The temperature dependence of the parameter a shown in Fig. 4(c) only confirms the small spread of the decay rates of the $j_{\mathrm{sc}}(B_{\mathrm{sc}})$ dependences observed in Fig. 3(b). Surprisingly, for a wide range of temperatures, 20–60 K, a is nearly tem-

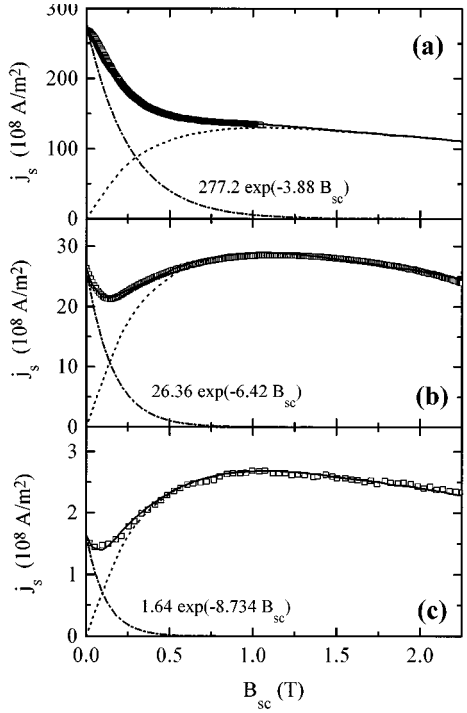

FIG. 8. Comparison of the experimental $j_s(B_{sc})$ data (symbols) with the modeled MHL (solid line) for $T=$ 7 K (a), 40 K (b), and 70 K (c). The modeled MHL was composed as a sum of the universal curve, Eq. (4) for $m=1$ and $n=0.5$ (dotted concave line), and the central peak contribution, Eq. (7) with parameters from fig. 4 (dot-dashed convex line). For sake of direct comparability with the measured current densities j_s the scaled current data obtained from Eqs. (4) and (7) were multiplied by $j_p(T)$ (see Fig. 4). For all investigated temperatures the solid line of the modeled curve coincides within the experimental error with the experimental data.

perature independent. Above 60 K the processes connected with the vortex lattice melting evidently start to play a significant role.

To manifest an applicability of our model in a wide range of temperatures, we make an inverse procedure to the above-described separation process. We add the universal curve, Eq. (4), and the functional description of the central peak [Eq. (7)] with parameters obtained from Fig. 4. Results of such procedures performed for 7 K, 40 K, and 70 K are shown in Figs. 8(a)–8(c) along with the corresponding experimental data. It is evident that the same superposition is able to model the whole process of the fishtail development starting from the classical MHL shape, with the continuously decreasing size [Fig. 8(a)], up to the MHL with a fully developed fishtail shape [Fig. 8(c)]. It confirms that the fishtail effect in samples like the ours can be understood as an overlapping of two separate pinning mechanisms with different temperature dependences. These mechanisms exist most probably also in samples which do not explicitly exhibit the fishtail ''anomaly.'' We believe that if we were able to suppress the central peak in such samples, we could observe there a fishtail deformation of the MHL, too.

D. Conclusions

The concept outlined above gives an answer to several fundamental features of the fishtail problem in R-Ba-Cu-O ($R\equiv$rare earth) single crystals.

(i) The fishtail effect occurs in different samples at different temperatures and fields: As discussed above, the fishtail phenomenon is a result of the interplay of two different pinning regimes. The separation process of both maxima in the $j_s(B)$ dependence [the high-field (fishtail) one and the central (low-field) one] with increasing temperature reflects developments of the actual shapes of the both contributions with temperature which differ from sample to sample. For instance, the reduction of the oxygen content[6] brings about the introduction of additional pinning sites (oxygen vacancies) which enhance critical currents in the high-field part of the MHL and increase probably also B_{c2}. As a result, the whole high-field part expands to higher fields and the fishtail maximum separates from the central peak.

(ii) Position of the fishtail *maximum* scales with $(1-T/T_c)^{1.37}$ which may have a link to the temperature dependence of the penetration depth[25] $\lambda(T)\propto(1-T/T_c)^{-1/2}$. It is most probable that just the change of λ with temperature sets the effective scale on the applied field. However, even in the scaled plot the fishtail *minimum* shifts to lower fields with increasing temperature. No scaling law for the position of the minimum has been yet found. The model presented here gives a natural explanation to it: The fishtail minimum shifts along the positive slope of the universal curve describing the high-field pinning mechanism in correspondence with the reduction of the central peak size with increasing temperature. The minimum results as a superposition of two contributions with different temperature dependences; it is easy to understand the difficulty of finding a simple analytical function describing the position of the minimum in such a case.

(iii) The fishtail effect is not observed at low temperatures: The central peak is sufficiently wide to mask the drop of the high-field pinning regime at fields close to zero.

Our relaxation measurements confirm a close correlation between the relaxation rate and the shape of the magnetic hysteresis loop which has been empirically established by Caplin *et al.*[26] and Perkins *et al.*[11,14] The analysis of the experimental $S(B)$ dependence indicates that the crossover effect in the form defined in Ref. 9 and the matching effect[3] can be excluded from the potential explanations of the fishtail effect.

The concept presented in this paper brings into accord both the static and dynamic approaches to the problem and the related experiments. The scenario of two independent pinning regimes points to the necessity of a better understanding of the vortex dynamics connected with the formation of the central peak of MHL's and of the flux motion in a diluted vortex lattice. Generation of self-fields, local field inhomogeneities, bending of vortices at nonzero transversal fields, surface barrier, and other effects can play a significant role here. The authors believe that this phenomenological analysis will be a challenge for theorists to build up a satisfactory theoretical microphysical background for the processes connected with the vortex dynamics in the central peak region which are most probably crucial for the fishtail minimum occurrence.

Note added. Very recently Abulafia *et al.* have published a paper[27] discussing the fishtail maximum in an Y-Ba-Cu-O

single crystal at temperature $T=85$ K close to T_c of this material. The authors attribute the maximum to the crossover between the elastic and plastic vortex creep with quite convincing arguments, giving in this way straightforward physical meaning (at least in the temperature range they study) to the field B_p used in this paper for normalization of the field scale at all temperatures. However, the theoretical temperature dependence of B_p following from the plastic creep model used in Ref. 27 gives, when extrapolated to low temperatures, values of the fishtail maximum position inconsistently high in comparison with the experimental ones. We believe that our paper will provoke further detailed study of the flux dynamics around the fishtail maximum in a wide temperature range.

ACKNOWLEDGMENTS

The authors appreciate fruitful discussions with A. J. J. van Dalen (Free University of Amsterdam, at present Argonne National Laboratory, Argonne, Illinois). This work was partly supported by the GA of the Czech Republic (Grant No. 202/93/0669) and GA ASCR (Grant No. A 1010512).

[1] T. G. Berlincourt *et al.*, Phys. Rev. Lett. **6**, 671 (1961).
[2] J. Petermann, Z. Metallk. **61**, 724 (1970).
[3] W. Buckel, *Supraleitung* (Akademie-Verlag, Berlin, 1973), and references therein.
[4] Y. Yeshurun, N. Bontemps, L. Burlachkov, and A. Kapitulnik, Phys. Rev. B **49**, 1548 (1994); K. A. Delin, T. P. Orlando, E. J. McNiff, Jr., S. Foner, R. B. van Dover, L. F. Schneemeyer, and J. V. Waszczak, *ibid.* **46**, 11 092 (1992); L. F. Cohen, J. R. Laverty, A. D. Caplin, and W. Assmus, Cryogenics **33**, 352 (1993); M. Werner, F. M. Sauerzopf, H. W. Weber, B. D. Vael, F. Licci, K. Winzer, and M. R. Koblischka, Physica C **235-240**, 2833 (1994); A. A. Zhukov *et al.*, Phys. Rev. B **52**, 9871 (1995).
[5] M. Däumling, J. M. Seuntjens, and D. C. Larbalestier, Nature **346**, 332 (1990); M. S. Osofsky, J. L. Cohn, E. F. Skelton, M. M. Miller, R. J. Soulen, Jr., S. A. Wolf, and T. A. Vanderah, Phys. Rev. B **45**, 4916 (1992).
[6] J. L. Vargas and D. C. Larbalestier, Appl. Phys. Lett. **60**, 1741 (1992).
[7] M. Jirsa, A. J. J. van Dalen, M. R. Koblischka, G. Ravi Kumar, and R. Griessen, in *Critical Currents in Superconductors*, edited by H. W. Weber (World Scientific, Singapore, 1994), p. 221.
[8] R. Hiergeist, R. Hergt, A. Erb, and G. Müller-Vogt, in *Critical Currents in Superconductors*, edited by H. W. Weber (World Scientific, Singapore, 1994), p. 225.
[9] L. Krusin-Elbaum, L. Civale, V. M. Vinokur, and F. Holtzberg, Phys. Rev. Lett. **69**, 2280 (1992).
[10] M. Ullrich, D. Müller, K. Heinemann, L. Niel, and H. C. Freyhardt, Appl. Phys. Lett. **63**, 406 (1993).
[11] G. K. Perkins, L. F. Cohen, A. A. Zhukov, and A. D. Caplin, Phys. Rev. B **51**, 8513 (1995).
[12] A. J. J. van Dalen, M. R. Koblischka, R. Griessen, M. Jirsa, and G. Ravi Kumar, Physica C **250**, 265 (1995).
[13] H. Schnack, R. Griessen, J. G. Lensink, C. J. van der Beek, and P. H. Kes, Physica C **197**, 337 (1992).
[14] G. K. Perkins and D. Caplin, Phys. Rev. B **54**, 12551 (1996).
[15] V. G. Hadjiev, C. Thomsen, A. Erb, G. Müller-Vogt, M. R. Koblischka, and M. Cardona, Solid State Commun. **80**, 643 (1991).
[16] C. P. Bean, Rev. Mod. Phys. **36**, 31 (1964).
[17] L. D. Landau, E. M. Lifshitz, and L. P. Pitaevskii, *Electrodynamics in Continuous Media*, 2nd ed. (Pergamon Press, Oxford, 1984), p. 185; V. F. Elesin, I. V. Zakharchenko, A. A. Ivanov, A. P. Menushenkov, A. A. Sinchenko, and S. V. Shavkin, Supercond. Phys. Chem. Technol. **3**, 1376 (1990).
[18] L. Klein, E. R. Yacoby, Y. Yeshurun, A. Erb, G. Müller-Vogt, V. Breit, and H. Wühl, Phys. Rev. B **49**, 4403 (1994); R. Prozorov, A. Tsaremet, Y. Yeshurun, G. Koren, M. Konczykowski, and S. Bouffard, Physica C **234**, 311 (1994); M. Kiuchi, E. S. Otabe, T. Matsushita, T. Kato, T. Hikata, and K. Sato, *ibid.* **260**, 177 (1996).
[19] L. Půst, J. Kadlecová, M. Jirsa, and S. Durčok, J. Low Temp. Phys. **78**, 179 (1990).
[20] M. Jirsa, L. Půst, H. G. Schnack, and R. Griessen, Physica C **207**, 85 (1993).
[21] According to the analysis in Refs. 11 and 14 determination of m from the experiment is much more straightforward and reliable than estimation of n. Therefore, we set $m=1$, in accordance with analysis of our relaxation data, and left only n as a variable.
[22] A. P. Malozemoff and P. A. Fisher, Phys. Rev. B **42**, 6784 (1990).
[23] M. Däumling *et al.*, Phys. Rev. B **50**, 1302 (1994); M. Däumling, E. Walker, G. Grasso, and R. Flükiger (unpublished).
[24] A. A. Zhukov, H. Küpfer, H. Claus, H. Wühl, M. Kläser, and G. Müller-Vogt, Phys. Rev. B **52**, R9871 (1995)
[25] T. Ishida and H. Mazaki, Jpn. J. Appl. Phys. **26**, L2003 (1987).
[26] A. D. Caplin, L. F. Cohen, G. K. Perkins, and A. A. Zhukov, Supercond. Sci. Technol. **7**, 412 (1994).
[27] Y. Abulafia, A. Shaulov, Y. Wolfus, R. Prozorov, L. Burlachkov, Y. Yeshurun, D. Majer, E. Zeldov, H. Wühl, V. B. Geshkenbein, and V. M. Vinokur, Phys. Rev. Lett. **77**, 1596 (1996).